Adhesive and Mammalian Transglutaminase Substrate Properties of *Candida albicans* Hwp1

Janet F. Staab,[1] Steven D. Bradway,[2]* Paul L. Fidel,[3] Paula Sundstrom[1]†

The pathogenesis of candidiasis involves invasion of host tissues by filamentous forms of the opportunistic yeast *Candida albicans*. Morphology-specific gene products may confer proinvasive properties. A hypha-specific surface protein, Hwp1, with similarities to mammalian small proline-rich proteins was shown to serve as a substrate for mammalian transglutaminases. *Candida albicans* strains lacking Hwp1 were unable to form stable attachments to human buccal epithelial cells and had a reduced capacity to cause systemic candidiasis in mice. This represents a paradigm for microbial adhesion that implicates essential host enzymes.

Candida albicans causes severe oropharyngeal and esophageal mucositis in patients with human immunodeficiency virus and hematogenously disseminated disease in iatrogenically compromised hosts (*1*). Loss of immune host defenses is primarily responsible for susceptibility to opportunistic candidiasis arising from endogenous *C. albicans* in the normal flora. However, proadhesive and proinvasive factors of *C. albicans* contribute to disease by mediating penetration of host tissues. Filamentous forms, particularly true hyphae, embed themselves within the superficial, keratinized layer of stratified squamous epithelium and grow by apical extension (*2*). True hyphae are extensions of germ tubes that emerge from yeasts. To explore the role of surface proteins in tissue invasion, we studied the function of *HWP1*, a developmentally regulated gene expressed in germ tubes and true hyphae (*2*). *HWP1* encodes an outer mannoprotein, Hwp1, with a cell surface–exposed NH_2-terminal domain and COOH-terminal features conferring covalent integration into cell wall β-glucan (*2*, *3*).

Unlike most pathogens that form various types of weak interactions with host cells, *C. albicans* germ tubes form nondissociable complexes with human buccal epithelial cells (BECs) that are characteristic of transglutaminase (TGase)-mediated reactions in stability and in being prevented by TGase inhibitors (*4*). A possible role for Hwp1 in formation of stable complexes with BECs was suggested by the amino acid sequence of the NH_2-terminal domain, which resembles mammalian TGase substrates (*2*), particularly the head and central domains of small proline-rich (SPR) proteins (*5*). Perhaps Hwp1 contributes to proliferation of *C. albicans* in keratinized epithelium by interacting with keratinocyte TGases (*6*), enzymes that create a host barrier defense by cross-linking SPR proteins and other proteins through covalent N^{ϵ}-(γ-glutamyl)lysine isodipeptide bonds. Cross-linking of epithelial cell proteins is essential. Mice lacking keratinocyte TGase die within a few hours of birth (*7*).

To determine if the SPR-like region of Hwp1 is a substrate for TGase, we examined a recombinant protein, rHwp1ΔC37, that encompasses the NH_2-terminal proline- and glutamine-rich domain (*8*) for the ability to incorporate [^{14}C]putrescine in the presence of TGase2. TGase2, also known as tissue TGase, is widely distributed in the body and is commonly used to characterize TGase substrates (*9*, *10*). Levels of radioactivity associated with the recombinant protein were equivalent to those of casein, a known TGase substrate, and were fourfold greater than for bovine serum albumin (BSA), a negative control (Fig. 1A). Examination of proteins after TGase reactions (Fig. 1, B and C) showed no radioactivity associated with BSA; however, the recombinant protein was similar to other TGase2 substrates in the generation of multiple species of radiolabeled reaction products including monomers displaying increased migration (*11*), species of high molecular weight (*10*, *12*), and dimers bridged by putrescine. The production of all radiolabeled forms depended on the presence of active TGase. In addition to [^{14}C]putrescine, TGase2 catalyzed the incorporation of another TGase cosubstrate, monodansylcadaverine (*13*), into rHwp1ΔC37 (*14*). The behavior of rHwp1ΔC37 in interactions with TGase2 matched that of SPR proteins and other host TGase substrates and implicated the NH_2-terminus of Hwp1 in cross-linking reactions with primary amines through N^{ϵ}-(γ-glutamyl)lysine isodipeptide bonds.

To study the TGase substrate properties of native Hwp1 on germ tube surfaces, we created isogenic strains with or without Hwp1 (*15*) for comparison in TGase assays. Disruption of *HWP1* was verified by Southern (DNA) and Northern (RNA) blotting (Fig. 2). CAH7-1A lacked *HWP1* mRNA (Fig. 2C) and protein (*16*), whereas heterozygous and complemented strains, CAH7 and CAHR3, had about half the amount of *HWP1* mRNA found in strains with unaltered *HWP1* genes,

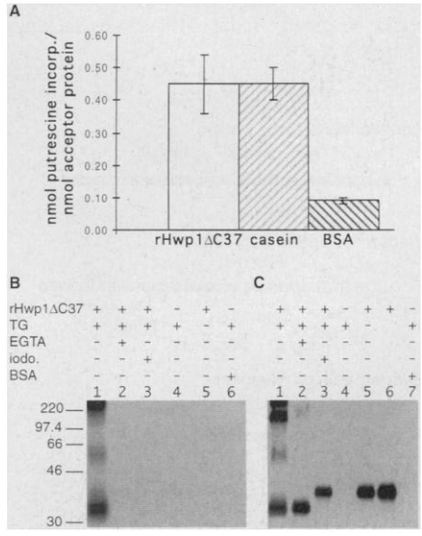

Fig. 1. (**A**) Incorporation of [^{14}C]putrescine by rHwp1ΔC37, casein, and BSA mediated by TGase (*25*). The values are the means (±SD) of two experiments performed in triplicate. (**B**) Autoradiograph of reactions with rHwp1ΔC37, [^{14}C]putrescine, and TGase after SDS–polyacrylamide gel electrophoresis and fluorography (*26*, *27*). Labeled products were not formed when reactions were supplemented with TGase inhibitors (*24*), including 20 mM EGTA to chelate Ca^{2+} (lane 2) and 20 mM iodoacetamide (lane 3), or in the absence of TGase (lane 5) or rHwp1ΔC37 (lane 4). Control reactions lacking putrescine showed that formation of the 59-kD species represented dimeric rHwp1ΔC37 bridged by putrescine (*14*). (**C**) Immunoblotting to detect rHwp1ΔC37 in TGase reactions with affinity-purified rabbit antibodies to rHwp1 (*2*, *28*) and horseradish peroxidase–conjugated goat antibodies to rabbit immunoglobulin G (Zymed), developed with ECL reagents (Amersham). Lane 6, rHwp1ΔC37 alone. TG, Tgase; iodo., iodoacetamide.

[1]Department of Medical Microbiology and Immunology, College of Medicine and Public Health, [2]Department of Periodontology, College of Dentistry, Ohio State University, 333 West Tenth Avenue, Columbus, OH 43210, USA. [3]Department of Microbiology, Immunology, and Parasitology, Louisiana State University Medical Center, 1901 Perdido Street, New Orleans, LA 70112, USA.

*Present address: Grays Harbor Dental Specialists, 105 South Broadway, Aberdeen, WA 98520, USA.

†To whom correspondence should be addressed. E-mail:sundstrom.1@osu.edu

although the amount of Hwp1 was indistinguishable from that of wild-type strains (*14*). Germ tubes of strains with one or both copies of *HWP1* displayed equivalent levels of TGase2 substrates, whereas parent blastoconidia were negative (Fig. 3A). Identical results were found with four clinical isolates of *C. albicans* from dental patients, and with other laboratory strains of *C. albicans* (*14*). TGase substrates were not detected in the presence of EGTA (Fig. 3A) or iodoacetamide, nor was endogenous TGase activity of *C. albicans* detected in whole organisms or in broken cell walls (*14*). In contrast to strains with Hwp1, TGase substrates were not detectable on germ tubes of the homozygous *hwp1/hwp1* mutant CAH7-1A (Fig. 3A), indicating the requirement of Hwp1 for TGase substrate activity. Thus, the NH_2-terminal domain of native Hwp1 appears to be a surface-exposed TGase substrate available for interactions with exogenous mammalian TGases.

If Hwp1 proteins serve as connections to BECs through interactions with TGases, then the stable attachments described previously (*4*) should be greatly reduced in strains lacking Hwp1. To test this hypothesis, we compared isogenic strains with or without Hwp1 in stabilized adhesion assays, which involved treatment of germ tube:BEC complexes with heat and the anionic detergent SDS to dissociate weak, noncovalent bonds (*4*, *17*). Strains with one or both copies of *HWP1* displayed equivalent levels of stabilized adhesion (Fig. 3B), indicating a lack of gene copy number effect and correlating well with apparent wild-type levels of Hwp1 protein and TGase substrates on germ tubes in these strains (Fig. 3A). Stabilized adhesion was prevented by monodansylcadaverine, a competitive inhibitor of TGase-mediated protein cross-linking reactions (*13*, *18*), and by iodoacetamide, supporting the involvement of BEC TGases (Fig. 3B). The *hwp1/hwp1* mutant strain CAH7-1A was greatly impaired in the ability to form stable attachments to BECs in that stabilized adhesion was only 23% of the other strains and was equivalent to values for other strains when TGase inhibitors were added. To provide further support for the role of Hwp1 in mediating stabilized adhesion, we radiolabeled rHwp1ΔC37 and incubated it with BECs in the presence or absence of iodoacetamide followed by treatment with heat and SDS (*19*). The results were consistent with stabilized adhesion assays in that rHwp1ΔC37 associated with BECs was sixfold greater when TGase was not inhibited. Adhesion of the control protein, BSA, was minimal (Fig. 3D). We have not identified the BEC TGases and TGase sub-

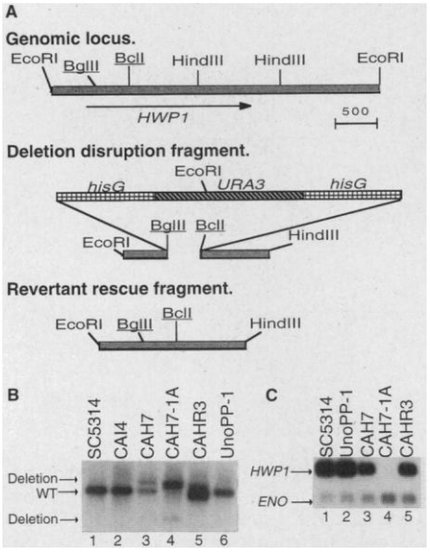

Fig. 2. Disruption of *HWP1* (*15*). (**A**) Genomic *HWP1* DNA open reading frame (arrow), plasmid insert of pGBHWP1 (shaded rectangle), disruption fragment from pHWP1URA3, and the rescue fragment (1.7 kb). (**B**) Southern blot of Eco RI–digested genomic DNA probed with the rescue fragment; *HWP1/HWP1*(SC5314, CAI4, and UnoPP-1) (3.8 kb) (lanes 1, 2, and 6), *hwp1/HWP1* (CAH7) (3.8, 5.3, and 2.3 kb) (lane 3), *hwp1/hwp1* (CAH7-1A) (5.3 kb, 5.1-kb doublet, and 2.3 kb) (lane 4), revertant CAHR3 (5.1 and 3.8 kb, 3.7-kb doublet) (lane 5). (**C**) Northern blot probed with *HWP1* and *ENO* (internal control) (*2*). Although CAHR3 harbored excess *HWP1* DNA (3.7-kb fragment), *HWP1* mRNA levels [quantified with ImageQuant Software (Molecular Dynamics)] were equivalent to those of CAH7, and developmental regulation was preserved.

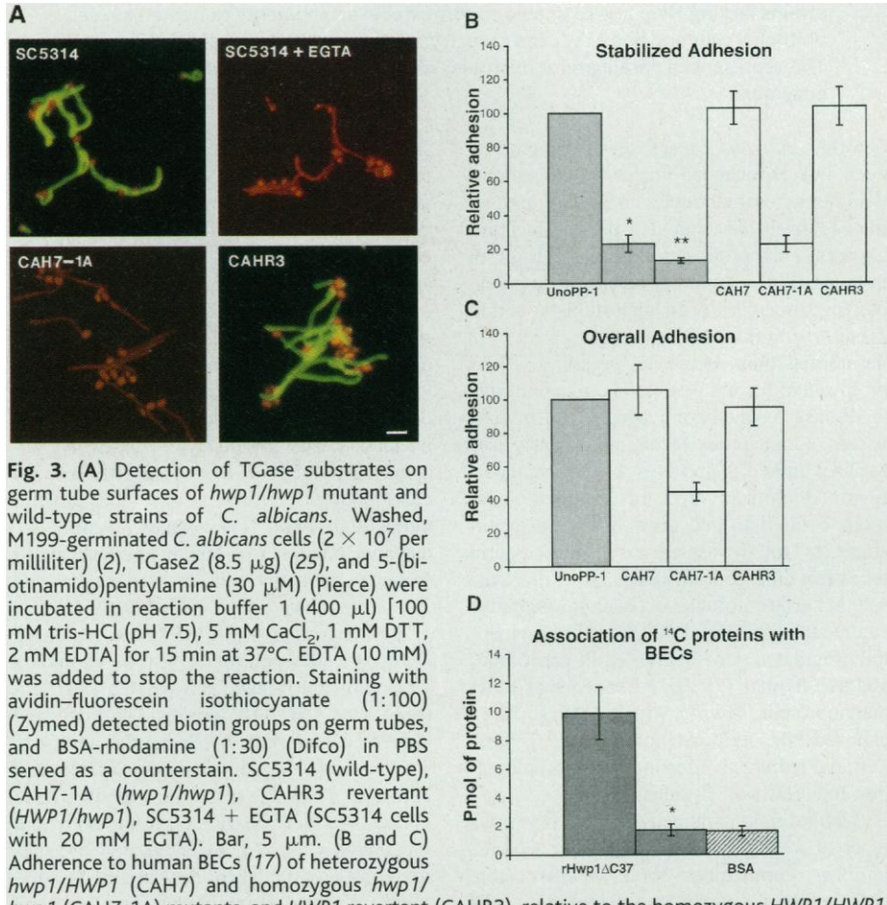

Fig. 3. (**A**) Detection of TGase substrates on germ tube surfaces of *hwp1/hwp1* mutant and wild-type strains of *C. albicans*. Washed, M199-germinated *C. albicans* cells (2×10^7 per milliliter) (*2*), TGase2 (8.5 μg) (*25*), and 5-(biotinamido)pentylamine (30 μM) (Pierce) were incubated in reaction buffer 1 (400 μl) [100 mM tris-HCl (pH 7.5), 5 mM $CaCl_2$, 1 mM DTT, 2 mM EDTA] for 15 min at 37°C. EDTA (10 mM) was added to stop the reaction. Staining with avidin–fluorescein isothiocyanate (1:100) (Zymed) detected biotin groups on germ tubes, and BSA-rhodamine (1:30) (Difco) in PBS served as a counterstain. SC5314 (wild-type), CAH7-1A (*hwp1/hwp1*), CAHR3 revertant (*HWP1/hwp1*), SC5314 + EGTA (SC5314 cells with 20 mM EGTA). Bar, 5 μm. (B and C) Adherence to human BECs (*17*) of heterozygous *hwp1/HWP1* (CAH7) and homozygous *hwp1/hwp1* (CAH7-1A) mutants, and *HWP1* revertant (CAHR3), relative to the homozygous *HWP1/HWP1* strain [UnoPP-1, a CAI4 derivative made Ura^+ by disruption of an enolase gene with *URA3* (*20*)]. (**B**) Stabilized adhesion. Adherence of UnoPP-1 was set at 100%, corresponding to counts per minute of 3100 to 6200, resulting in germ tube BEC ratios of 1 to 2:1 in a typical experiment. Asterisks indicate the presence of iodoacetamide (*) and monodansylcadaverine (**). The values are the means (±SD) of two experiments performed in duplicate. Statistically significant differences were determined by Student's *t* test. CAH7-1A versus CAH7 ($P = 0.009$), CAH7-1A versus UnoPP-1 with iodoacetamide or monodansylcadaverine to inhibit TGase ($P = 0.936$ and 0.142, respectively), and CAHR3 versus CAH7 ($P = 0.977$). (**C**) Overall adhesion. CAH7-1A versus CAH7 ($P = 0.032$), and CAHR3 versus CAH7 ($P = 0.513$). (**D**) BEC envelope-associated [^{14}C]rHwp1ΔC37 after incubations under adhesion assay conditions (*19*) with (*) or without 10 mM iodoacetamide followed by boiling in sample buffer for 5 min. Results of two experiments performed in duplicate (±SD) are shown. Statistically significant differences were determined by Student's *t* test. Uninhibited samples versus samples with iodoacetamide ($P = 0.025$), rHwp1ΔC37 versus BSA ($P = 0.025$), and samples with iodoacetamide versus BSA ($P = 0.855$).

strates participating in interactions with *C. albicans*, but rHwp1ΔC37 forms stable attachments to BECs and Hwp1 is required for formation of stable complexes between *C. albicans* germ tubes and BECs.

Hwp1 had a minor effect on overall adhesion of germ tube:BEC complexes not subjected to heat and detergent treatments (Fig. 3C). Overall adhesion of CAH7-1A was 45% that of UnoPP-1, lower than the expected value of 65% on the basis of a stabilized to overall adhesion ratio of 35 ± 5.75% for UnoPP-1. Hwp1 may contribute to typical, noncovalent adhesive forces between germ tubes and BECs, but it is more likely that the primary role of Hwp1 is in the formation of stable attachments and that the in vitro assay does not permit maximal cross-linking of germ tubes to BECs. Hyphae complexed to human BECs in vivo in specimens of pseudomembranous candidiasis of the buccal mucosa were not dissociated by heat and detergent treatments (up to 30 min) used in the stabilized adhesion assays (*14*), indicating that stable attachments predominate in candidiasis. Long incubation periods (18 hours) are required for maximal cross-linking of SPR2 protein by epithelial cell TGase3 (*10*). The similarity of Hwp1 to SPR proteins suggests that interactions of BEC TGases with SPR proteins are indicative of interactions with Hwp1 and that the primary role of Hwp1 is in the formation of stable attachments.

The importance of Hwp1 in candidiasis is supported by experiments showing that, despite similar growth rates and germ tube production [(*15*) and Fig. 3A], CAH7-1A was a poor inducer of systemic candidiasis in mice (Fig. 4).

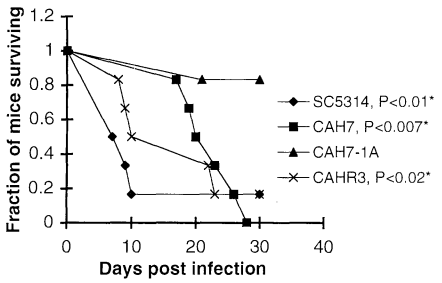

Fig. 4. Survival of mice (CBA/J H-2^k haplotype) intravenously injected with *HWP1* mutant strains. Four groups (six per group) of mice were injected with stationary-phase yeasts (*29*) (2×10^5 cells per mouse in 0.2 ml of PBS) of SC5314 (wild-type), CAH7 (*hwp1/HWP1*), CAH7-1A (*hwp1/hwp1*), or CAHR3 (*HWP1/hwp1*, revertant). The experiment was terminated at 30 days. The authenticity of strains taken from organs of infected mice was verified by assessment of the presence of Hwp1 on germ tubes by indirect immunofluorescence. Statistical analysis showed survival differences ($P < 0.01$) by the Wilcoxon rank sum test. (*) Significance of survival differences relative to the *hwp1/hwp1* strain, CAH7-1A, by the log rank test. Differences between strains expressing *HWP1* were not significant.

Of the six mice injected with CAH7-1A, five survived to the 30-day end point, two having cleared the infection. In the other groups, only 2 of 18 mice given *HWP1*-expressing strains survived. Colony-forming units of *C. albicans* were detected in homogenized brain, kidney, liver, and spleen of all infected animals, and numerous hyphae were found in the kidneys. CAH7-1A hyphae appeared less invasive in that organisms were limited to the renal pelvis, whereas other strains invaded the parenchyma (*14*). Thus, Hwp1 may promote internal candidiasis through TGases present in nonsuperficial tissues.

Germ tubes and hyphae of *C. albicans* exhibit highly polarized, apical growth and require mechanisms for anchoring within and penetration of host tissues. In mimicking mammalian TGase substrates, Hwp1 forms stable attachments between germ tubes and mammalian cells and is important in the pathogenesis of candidiasis.

References and Notes

1. C. J. Fichtenbaum and W. G. Powderly, *Clin. Infect. Dis.* **26**, 556 (1998); J. H. Rex, T. J. Walsh, E. J. Anaissie, *Adv. Int. Med.* **43**, 321 (1998).
2. J. F. Staab, C. A. Ferrer, P. Sundstrom, *J. Biol. Chem.* **271**, 6298 (1996).
3. J. F. Staab and P. Sundstrom, *Yeast* **14**, 681 (1998).
4. S. D. Bradway and M. J. Levine, *Crit. Rev. Oral Biol. Med.* **4**, 293 (1993).
5. S. J. Austin *et al.*, *J. Biol. Chem.* **271**, 3737 (1996).
6. U. Reichert, S. Michel, R. Schmidt, in *Molecular Biology of the Skin: The Keratinocyte*, M. Darmon and M. Blumenberg, Eds. (Academic Press, San Diego, CA, 1993), chap. 4, p. 107.
7. M. Matsuki *et al.*, *Proc. Natl. Acad. Sci. U.S.A.* **95**, 1044 (1998).
8. rHwp1ΔC37, encompassing the NH_2-terminus of the mature protein through the proline- and glutamine-rich-repeats [amino acids 40 to 197 encoded by *HWP1* cDNA (*2*)], was purified from culture media of *Pichia pastoris* by anion-exchange chromatography (Mono Q, Bio-Rad), with a salt gradient (0 to 1 M NaCl) in column buffer [50 mM tris-HCl (pH 8), 2 mM mercaptoethanol, 1 mM EDTA].
9. J. E. Folk, *Adv. Enzymol. Relat. Areas Mol. Biol.* **54**, 1 (1983).
10. E. Tarcsa *et al.*, *J. Biol. Chem.* **273**, 23297 (1998).
11. M. T. Kaartinen, A. Pirhonen, A. Linnala-Kankkunen, P. H. Maenpaa, *ibid.* **272**, 22736 (1997).
12. C. Barsigian, A. M. Stern, J. Martinez, *ibid.* **266**, 22501 (1991).
13. L. Lorand, O. M. Lockridge, L. K. Campbell, R. Myhrman, J. Bruner-Lorand, *Anal. Biochem.* **44**, 221 (1971); P. T. Velasco, F. Karush, L. Lorand, *Biochem. Biophys. Res. Commun.* **152**, 505 (1988); L. Lorand, L. K. Campbell-Wilkes, L. Cooperstein, *Anal. Biochem.* **50**, 623 (1972).
14. J. F. Staab and P. Sundstrom, data not shown.
15. W. A. Fonzi and M. Y. Irwin, *Genetics* **134**, 717 (1993). The *hisG-URA3-hisG* cassette from p5921 was inserted into pGBHWP1 (*2*), replacing 365 base pairs between Bgl II and Bcl I sites in the *HWP1* coding region, creating pHWP1URA3. Hind III–digested pHWP1URA3 was introduced into CAI4 to create a Ura$^+$ heterozygous *hwp1/HWP1* strain, CAH7. Ura$^-$ descendants of CAH7, selected on medium containing 5-fluoroorotic acid, were transformed with Hind III–digested pHWP1URA3, producing the homozygous *hwp1/hwp1* strain CAH7-1A. An *HWP1* revertant strain, CAHR3, was created by cotransformation of a Ura$^-$ homozygous *hwp1/hwp1* strain, CAH7-1A1, with Hind III–digested pGBHWP1 and p24enura (*20*) digested with Xba I–Xho I, resulting in an enolase gene disrupted with *URA3*. Generation times of CAH7, CAH7-1A, and CAHR3 were 2.52, 2.57, and 2.57 hours, respectively, whereas that of SC5314 was 2.00 hours in YNB at 27°C.
16. Hwp1 was assessed with monospecific antiserum to rHwp1 in indirect immunofluorescence assays (*2*).
17. Mass conversion of yeasts, radiolabeled with Tran^{35}S-label (ICN) (5 μCi/ml), to germ tubes (5×10^6 per milliliter) was induced in prewarmed M199 (40 ml) for 2.5 hours at 37°C, typically resulting in 3.11×10^5 cpm per 10^7 germ tubes. No differences in the proportion (>95%), length, or aggregation of germ tubes were found among strains. Single-cell suspensions of BECs were collected with a wooden applicator stick from the buccal surfaces of consenting healthy volunteers who understood the nature of the studies. Washed germ tubes and BECs, counted by hemacytometry, were mixed in 300 μl of reaction buffer 3 [50 mM tris-HCl (pH 7.5), 10 mM $CaCl_2$, 1 mM EDTA, 1 mM dithiothreitol (DTT)], at a germ tube/BEC ratio of 100:1 and incubated for 1 hour at 37°C, followed by reaction termination with 100 mM EGTA (75 μl). For overall adhesion, radioactivity of BEC fractions was determined by scintillation counting after centrifugation on 50% Percoll gradients (*21*), and the number of germ tubes per BEC was determined with the specific activity of each strain. For stabilized adhesion assays, reaction mixtures were heated to 100°C for 2 min in phosphate-buffered saline (PBS) containing 1% SDS before loading on Percoll gradients. Monodansylcadaverine (5 mM) or iodoacetamide (10 mM) was used to inhibit TGase during the 1-hour incubation at 37°C. Subtracted background counts, determined from gradients lacking BECs, were less than 6% of counts for BEC-associated counts. Visual counting confirmed results with radiolabeled cells.
18. L. Lorand *et al.*, *Biochemistry* **3**, 1214 (1968).
19. rHwp1ΔC37 (1 mg) was radiolabeled at the NH_2-terminus by incubation with a 200-fold molar excess of [^{14}C]acetic anhydride (Sigma, 6.4 mCi/mmol) in 0.4 M $NaHCO_3$ (pH 7.5), as described (*22*). [^{14}C]rHwp1ΔC37 (5.68 mCi/mmol) was equivalent to unlabeled protein in TGase substrate properties (*14*). Radiolabeled rHwp1ΔC37 or [^{14}C]BSA (Sigma) (1.2 nmol) was incubated with 10^5 BECs in 300 μl of reaction buffer 3 under stabilized adhesion assay conditions (*17*). BECs were washed in 500 μl of PBS, suspended in 50 μl of sample buffer (*23*), boiled for 5 min, vortexed, and centrifuged. Supernatants containing unbound proteins were discarded and BECs were suspended in PBS (50 μl) and transferred to vials with scintillation fluid to determine BEC-associated dpm.
20. P. Postlethwait and P. Sundstrom, *J. Bacteriol.* **177**, 1772 (1995).
21. W. C. Childs III and R. J. Gibbons, *J. Dent. Res.* **67**, 826 (1988).
22. B. Desbuquois, *Eur. J. Biochem.* **60**, 335 (1975).
23. U. K. Laemmli, *Nature* **227**, 680 (1970).
24. J. E. Folk and S. I. Chung, *Methods Enzymol.* **113**, 358 (1985).
25. rHwp1ΔC37 (10 μg) (*8*), *N,N′*-dimethylcasein (50 μg) (Sigma), or BSA (50 μg) (Fraction V, Sigma) was incubated with 250 nCi (2.2 to 2.3 nmol) of [^{14}C]putrescine (Amersham or DuPont/NEN, 108 to 110 mCi/mmol) and TGase2 (3.4 μg), prepared from guinea pig livers (*24*) (giving a change in fluorescence of 119 with a Perkin-Elmer LS-5B fluorometer in standard assays), in reaction buffer 2 [100 mM tris-HCl (pH 7.5), 20 mM $CaCl_2$, 1 mM DTT, 1 mM EDTA] for 30 min at 37°C (total volume, 25 μl). Radioactivity bound to acceptor proteins was assessed by scintillation counting after trichloroacetic acid precipitation. Background counts from reactions without acceptor proteins were subtracted from total counts (*13*).
26. Reactions (*25*) were incubated for 4 hours and quenched with cold putrescine (100 mM) for 1 hour before boiling in Laemmli sample buffer (*23*) for 5 min.
27. J. P. Chamberlain, *Anal. Biochem.* **98**, 132 (1979).
28. J. Sambrook, E. F. Fritsch, T. Maniatis, *Molecular Cloning: A Laboratory Manual* (Cold Spring Harbor Laboratory, Cold Spring Harbor, NY, 1989), pp. 18.17–18.18.
29. Organisms were grown for 18 hours in phytone-

peptone broth supplemented with 0.1% glucose at 25°C with shaking at 100 rpm.
30. Animal studies were conducted in accordance with the NIH guidelines for the care and use of laboratory animals. We thank A. Jackson for assistance with preparation of TGase2, B. Taylor for assistance with the animal experiments, and C. M. Allen for histological assessments of infected mouse tissues. Support for this research was provided from grant 1 R01 DE11375-05A2 from the National Institute of Dental and Craniofacial Research (P.S.) and AI32556 from the National Institute for Allergy and Infectious Diseases (P.L.F.).

30 October 1998; accepted 3 February 1999

The Predictive Value of Changes in Effective Connectivity for Human Learning

C. Büchel,* J. T. Coull, K. J. Friston

During learning, neural responses decrease over repeated exposure to identical stimuli. This repetition suppression is thought to reflect a progressive optimization of neuronal responses elicited by the task. Functional magnetic resonance imaging was used to study the neural basis of associative learning of visual objects and their locations. As expected, activation in specialized cortical areas decreased with time. However, with path analysis it was shown that, in parallel to this adaptation, increases in effective connectivity occurred between distinct cortical systems specialized for spatial and object processing. The time course of these plastic changes was highly correlated with individual learning performance, suggesting that interactions between brain areas underlie associative learning.

Studies of associative learning aim (i) to identify neural structures that constitute memory systems and (ii) to characterize the network properties that comprise interactions among their components. The first aim has been addressed largely by using functional neuroimaging, on the basis of the principle of functional specialization. In the case of object-location memory, several functional studies have demonstrated activation of ventral occipital and temporal regions during the retrieval of object identity and, conversely, increased responses in dorsal parietal areas during the retrieval of spatial location (*1*–*3*). These results suggest domain-specific representations in posterior neocortical structures, closely related to those involved in perception, and they accord with the segregation of ventral and dorsal pathways in processing categorical or spatial stimulus features, respectively (*4*). Another phenomenon observed in some learning studies is a decrease of neural responses (that is, adaptation) to repeated stimulus presentations. This repetition suppression has been replicated consistently in primate electrophysiological and human functional imaging studies (*5*). Although certainly not the only electrophysiological correlate of learning, it is ubiquitous and a useful measure of learning-related changes intrinsic to unit or population responses. For object-location learning, it is intuitively likely that two specialized systems need to interact to establish an association. Domain-specific representations or repetition suppression is not sufficient to account for this associative component (*6*). In other words, functional segregation and localized response properties cannot account for associative learning alone. Here, we address the functional integration of different systems to characterize learning from a different perspective, namely, that of effective connectivity (*7*).

Whole-brain functional magnetic resonance imaging (fMRI) was used to test the hypotheses that (i) repeated stimulus presentation during learning will lead to adaptation of evoked cortical responses (repetition suppression) and (ii) learning the association of two stimulus attributes that are processed in segregated cortical regions is accompanied by changes in effective connectivity between these regions over time. We chose object location and object identity as the two attributes to be associated because they are processed in the segregated dorsal and ventral visual pathways, respectively (*4*).

Six participants (three male and three female, age range 25 to 36) had to learn and recall the association between 10 simple line drawings of real-world objects and 10 locations on a screen during fMRI (*8*). Each learning trial consisted of four conditions, encoding (ENC), control-1 (CO1), retrieval (RET), and control-2 (CO2) (*9*) (Fig. 1A). The behavioral data acquired during RET demonstrated that all six individuals were able to learn the association between object identity and spatial location for all 10 objects within eight learning trials, as indicated by the ensuing asymptotic learning curves (Fig. 2A) (*10*).

Regionally specific changes in evoked responses over time were assessed by examining time-by-condition interactions (*11*). Decreases in activation during learning, indicative of repetition suppression, were observed in several cortical regions in the ventral and dorsal visual pathway (Fig. 2, B and C). Within the framework of repetition suppression it has been hypothesized that decreases in neural responses are epiphenomena of enhanced response selectivity (*5*). By analogy to the development and plasticity of cortical architectures (*12*), this refined selectivity is likely to be due to changes in effective connectivity within the system at a synaptic level. In this study we explicitly addressed this idea by characterizing time-dependent changes in effective connectivity during learning.

Path analysis was used to assess changes in effective connectivity between the dorsal and ventral pathways over time. This technique can be considered as a decomposition of interregional correlations, constrained by an underlying anatomical model. The resulting path coefficients are estimates of effective connectivity and represent the response, in units of standard deviation, of the dependent variable (activity in the target region) for a change of one standard deviation of the explanatory variable (activity in the source region), while activity elsewhere is held constant.

The regions of interest for the path analysis were selected from individual participant analyses of evoked responses (*13*). As expected for visual stimuli consisting of line drawings, we observed responses in striate (V1) and dorsal extrastriate (DE) visual cortex, posterior parietal cortex (PP), and lateral parietal cortex (LP). Ventrally, we found activation of posterior inferotemporal cortex (ITp) and, more anteriorly, in the parahippocampal gyrus (ITa) (Fig. 1B) (*14*).

Given our hypothesis regarding changes in effective connectivity between dorsal and ventral pathways, the path analysis was focused on the connection between PP (dorsal stream) and ITp (ventral stream). We tested changes in this path coefficient, over time within a session, by dividing each learning session into "Early" (first part) and "Late" observations (second part) and estimating separate path coefficients for each (Fig. 1A) (*15*).

The structural model used in our analysis embodies connections within and across ventral and dorsal pathways (Fig. 1B) and is based on anatomical studies in primates (*16*).

The Wellcome Department of Cognitive Neurology, Institute of Neurology, 12 Queen Square, London WC1N 3BG, UK.

*To whom correspondence should be addressed. E-mail: c.buechel@fil.ion.ucl.ac.uk